Electronic Supplementary Material (ESI) for Journal of Materials Chemistry C.

Supporting Information

Bio-inspired Micro Area Concentrated Array Assisted Perovskite Photodetector toward Weak Light Imaging

Lutong Guo [1,2], Kun Zhang[1,2], Mingquan Tao[1,2], Rudai Zhao[1], Tingqing Wu[1,2], Yang Wang[1,2] and Yanlin Song*[1,2]*

[1] Key Laboratory of Green Printing, Institute of Chemistry, Chinese Academy of Sciences, Beijing National Laboratory for Molecular Sciences, CAS Research/Education Center for Excellence in Molecular Sciences, Zhongguancun North First Street 2, 100190 Beijing (P. R. China)

[2] School of Chemical Science, University of Chinese Academy of Sciences, 100190 Beijing (P. R. China)

E-mail: wangyang@iccas.ac.cn; ylsong@iccas.ac.cn

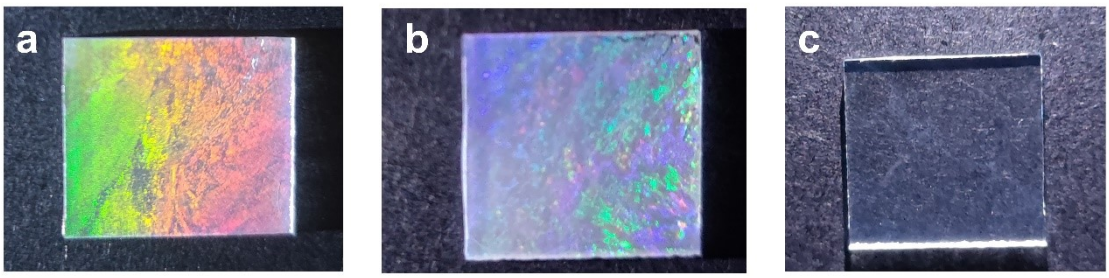

Figure S1. Photograph of (a) 600 nm-2D PC, (b) 900 nm-2D PC, (c) 180 nm-2D PC.

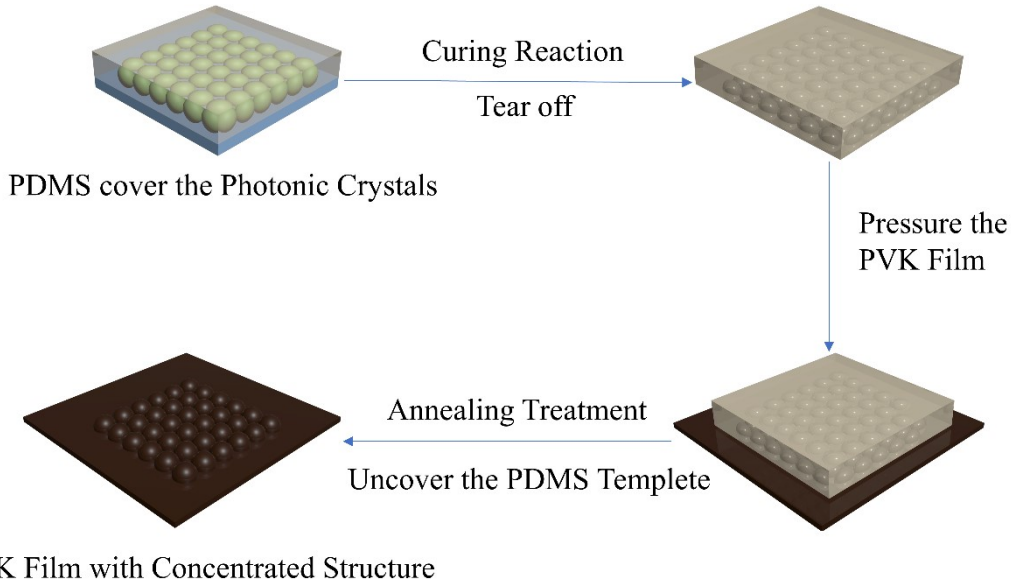

Figure S2. The preparation of the bio-inspired micro area concentrated perovskite.

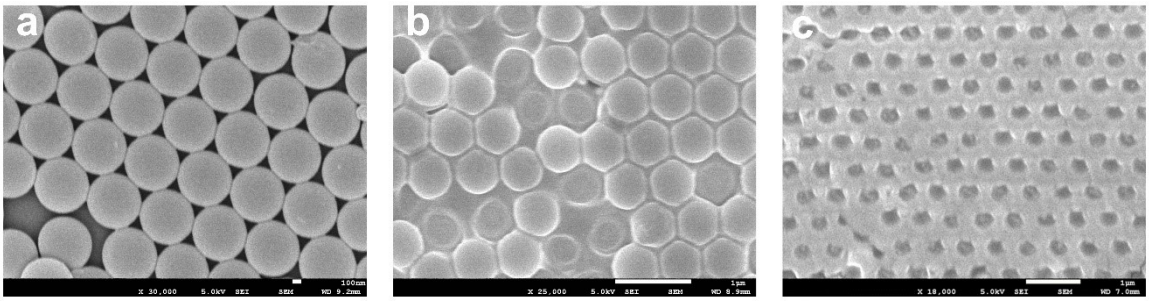

Figure S3. (a, b) SEM images of 600 nm-2D PC (a)before pouring PDMS and (b) after tearing off the PDMS bump stamp. (c) SEM images of 600 nm-PDMS bump stamp. Due to the force balance, the actual size of the hole is 2/3 of that of the ball.

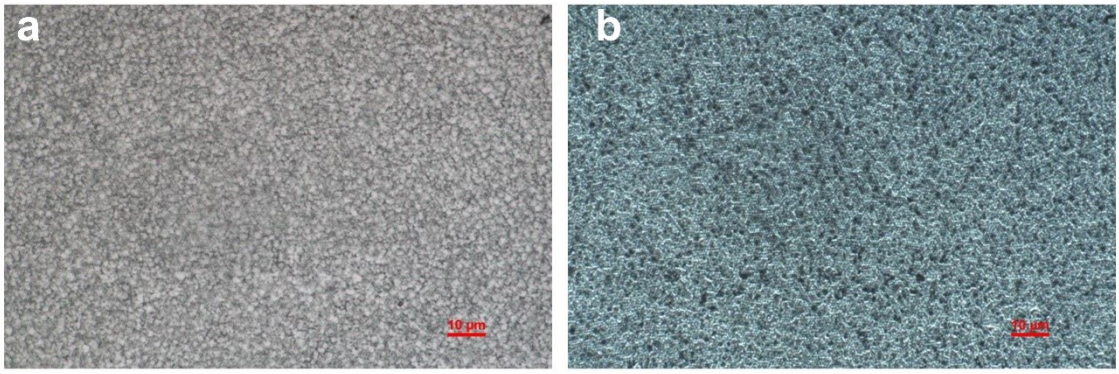

Figure S4. Optical microscopy of (a) brightfield and (b) darkfield photographs of the 600 nm-PVK.

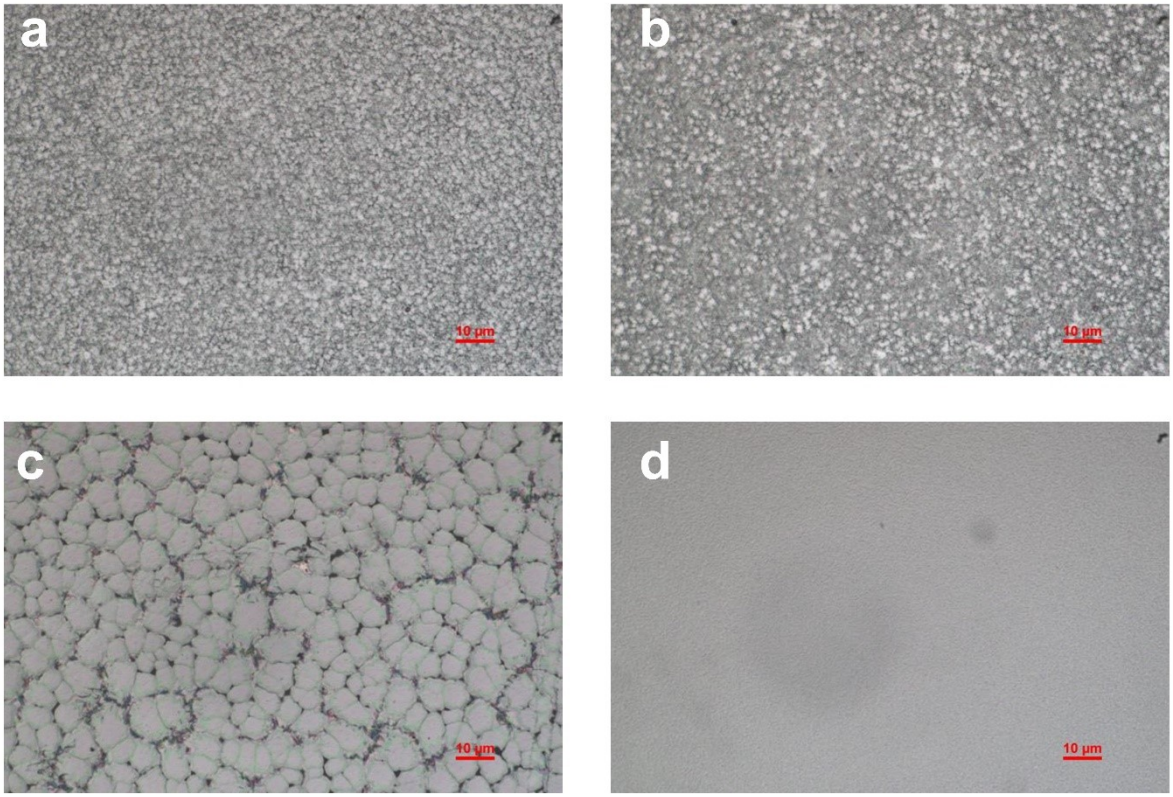

Figure S5. Optical microscopy brightfield photographs of (a) 600 nm-PVK, (b) 900 nm-PVK, (c) 180 nm-PVK and (d) Flat-PVK. Due to the small size of 180 nm, pressure-induced crystallization dominates and exhibits different crystallization behaviors.

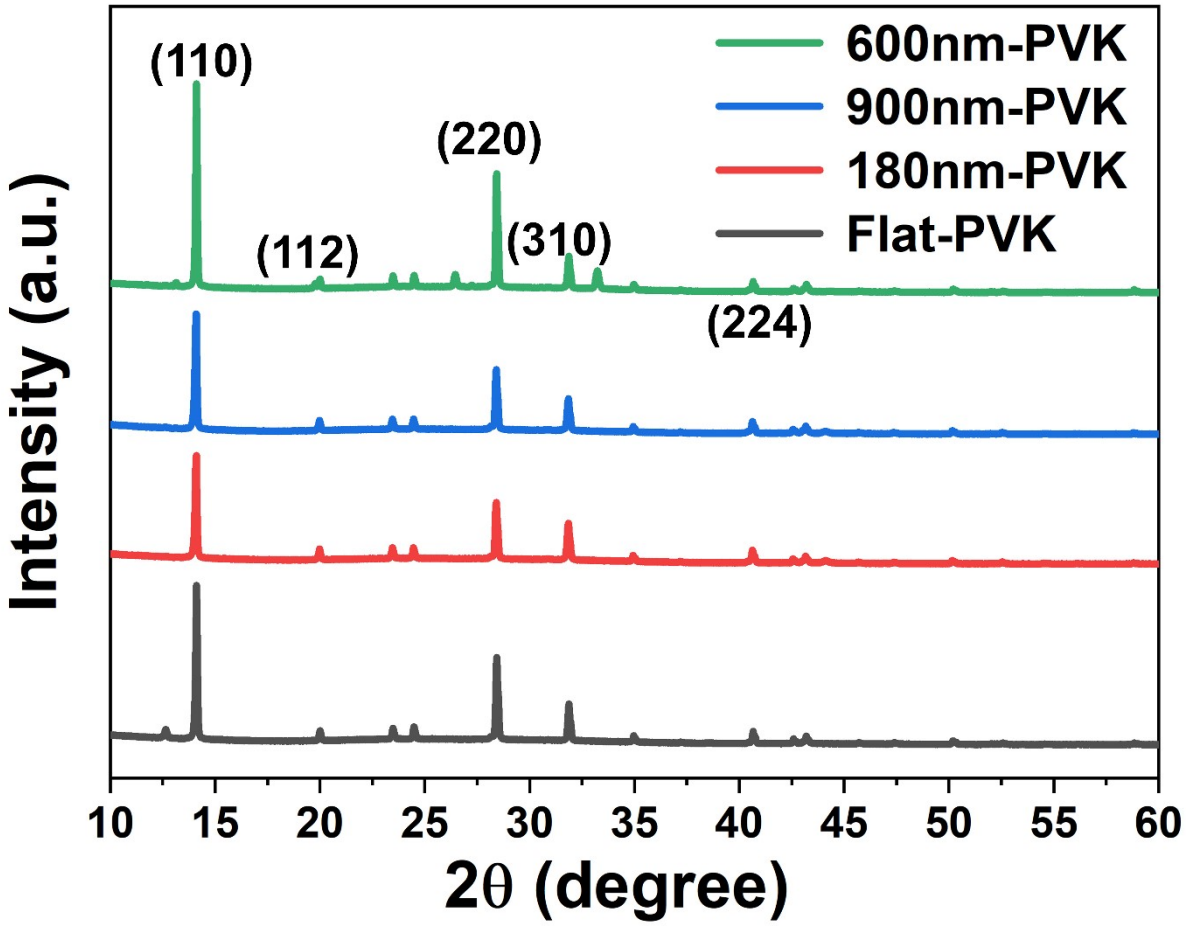

Figure S6. X-ray diffraction of 600 nm-PVK, 900 nm-PVK, 180 nm-PVK and Flat-PVK films. The XRD diffraction peaks of (110), (112), (220), (310), and (224) indicate that the samples have a pure tetragonal phase.

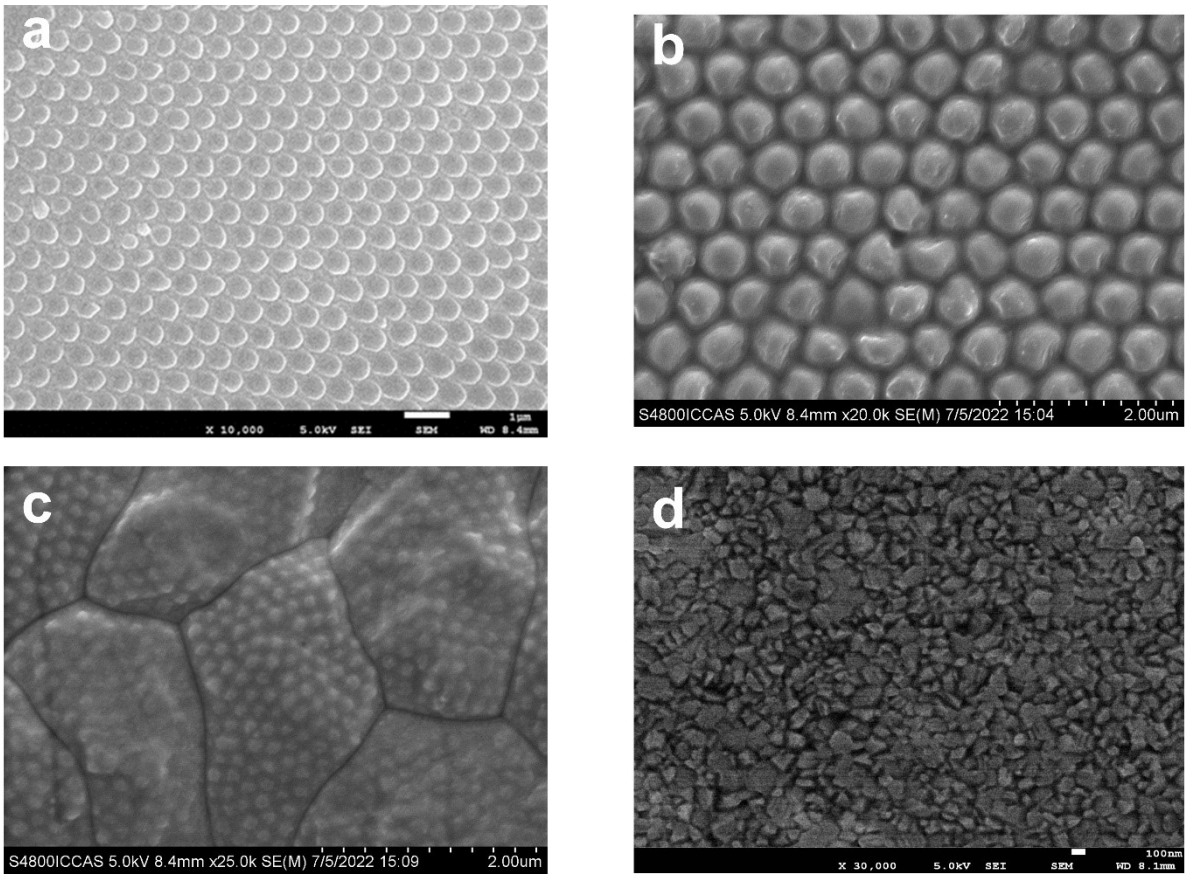

Figure S7. SEM images of (a) 600nm-PVK, (b) 900nm-PVK, (c) 180nm-PVK and (d) Flat-PVK. These results are consistent with optical microscopy results.

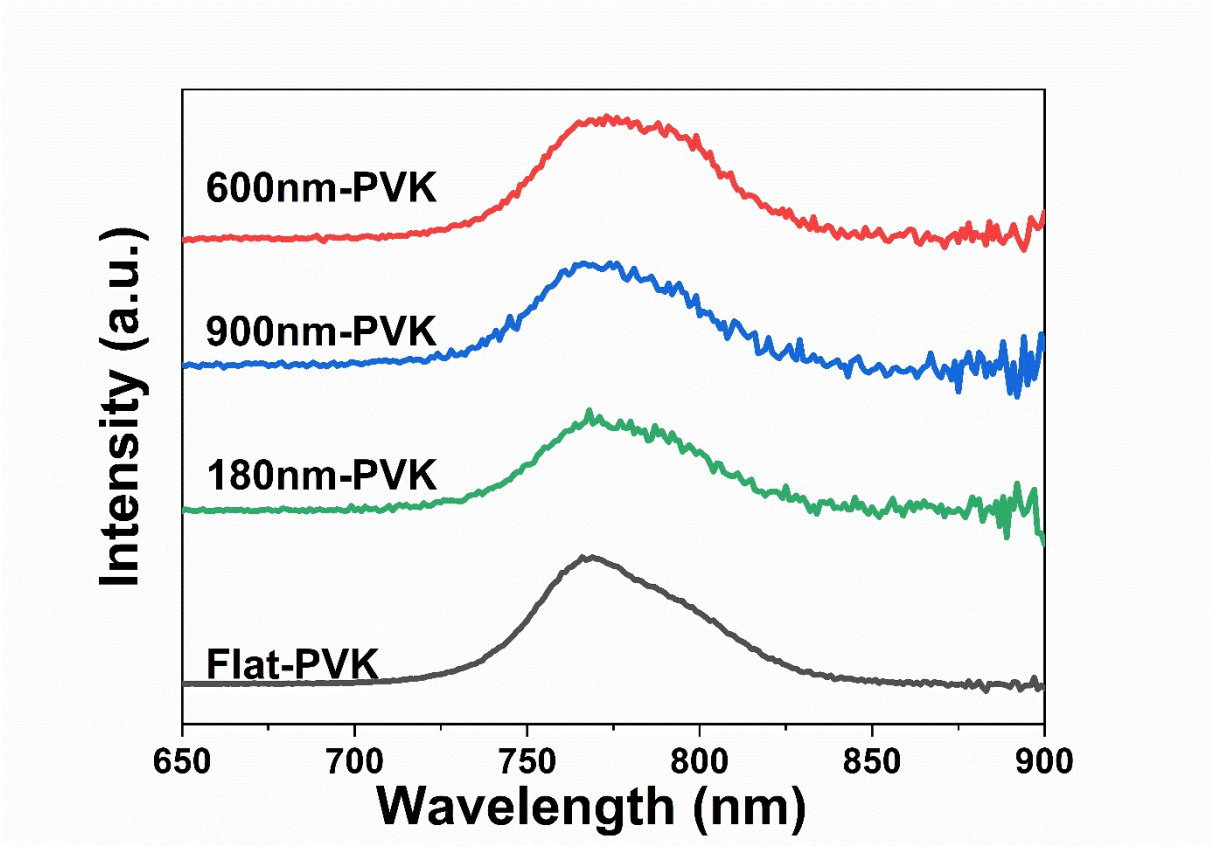

Figure S8. Steady-state photoluminescence of 600 nm-PVK, 900 nm-PVK, 180 nm-PVK and Flat-PVK films.

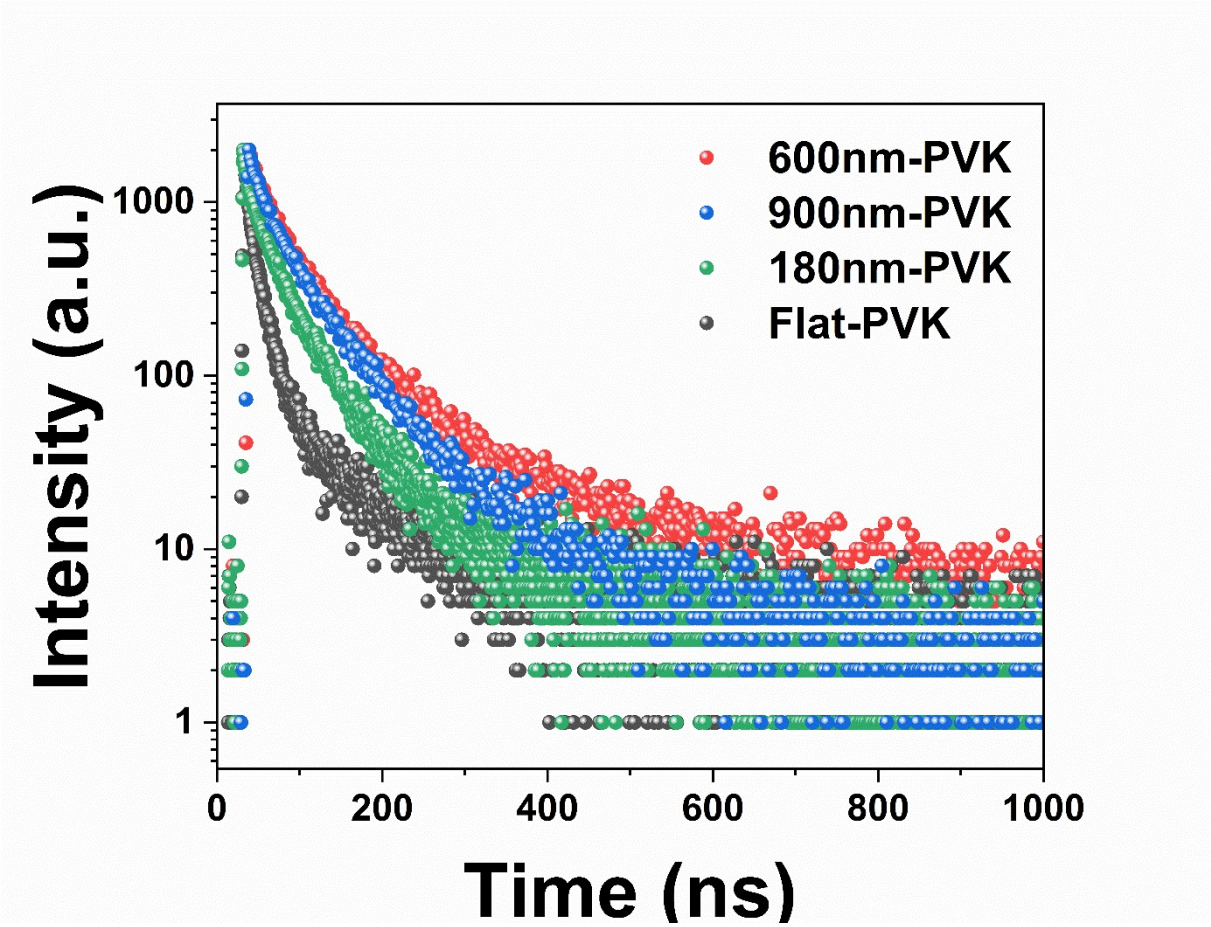

Figure S9. Time-resolved photoluminescence of 600 nm-PVK, 900 nm-PVK, 180 nm-PVK and Flat-PVK films, respectively. The 600nm-PVK film exhibits a minimum short-lived PL lifetime with nonradiative recombination and a maximum long-lived PL lifetime with radiative recombination

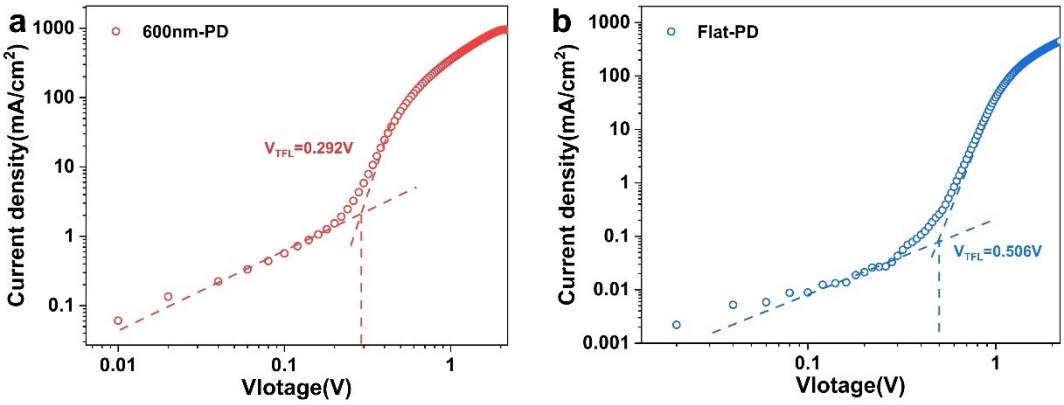

Figure S10. Current density-voltage characteristics of devices with FTO/perovskite /Au: (a) 600 nm-PD and (b) Flat-PD.

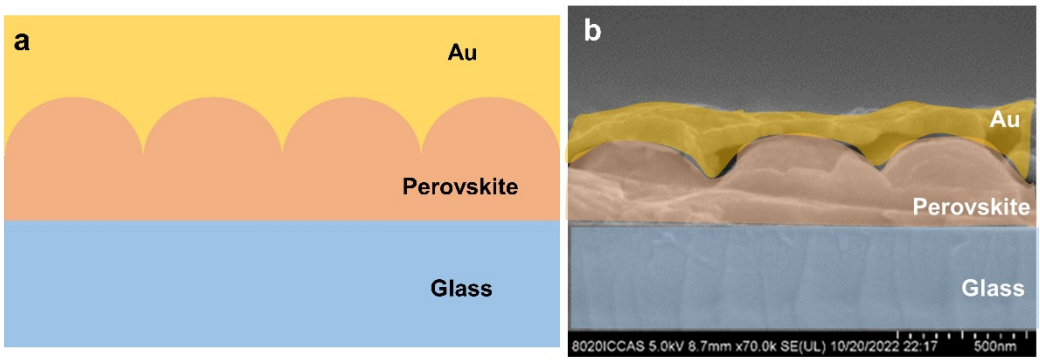

Figure S11. Diagram (a) and cross-sectional SEM image (b) of 600nm-PD device

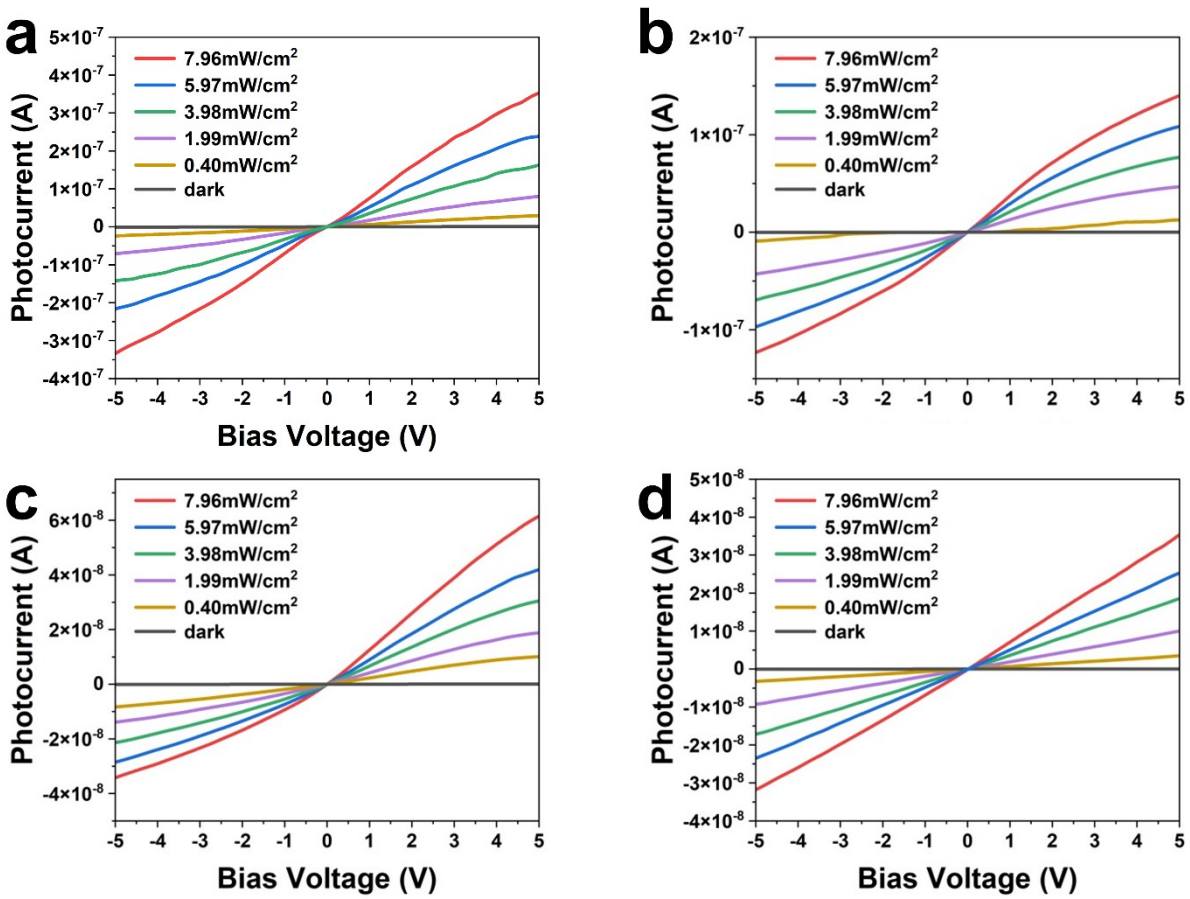

Figure S12. Photoelectric properties of perovskite photodetector. I-V curves of a) 600 nm-PD, b) 900 nm-PD, c) 180 nm-PD and d) Flat-PD in dark and under different light intensity, 650 nm light illumination at 5 V bias.

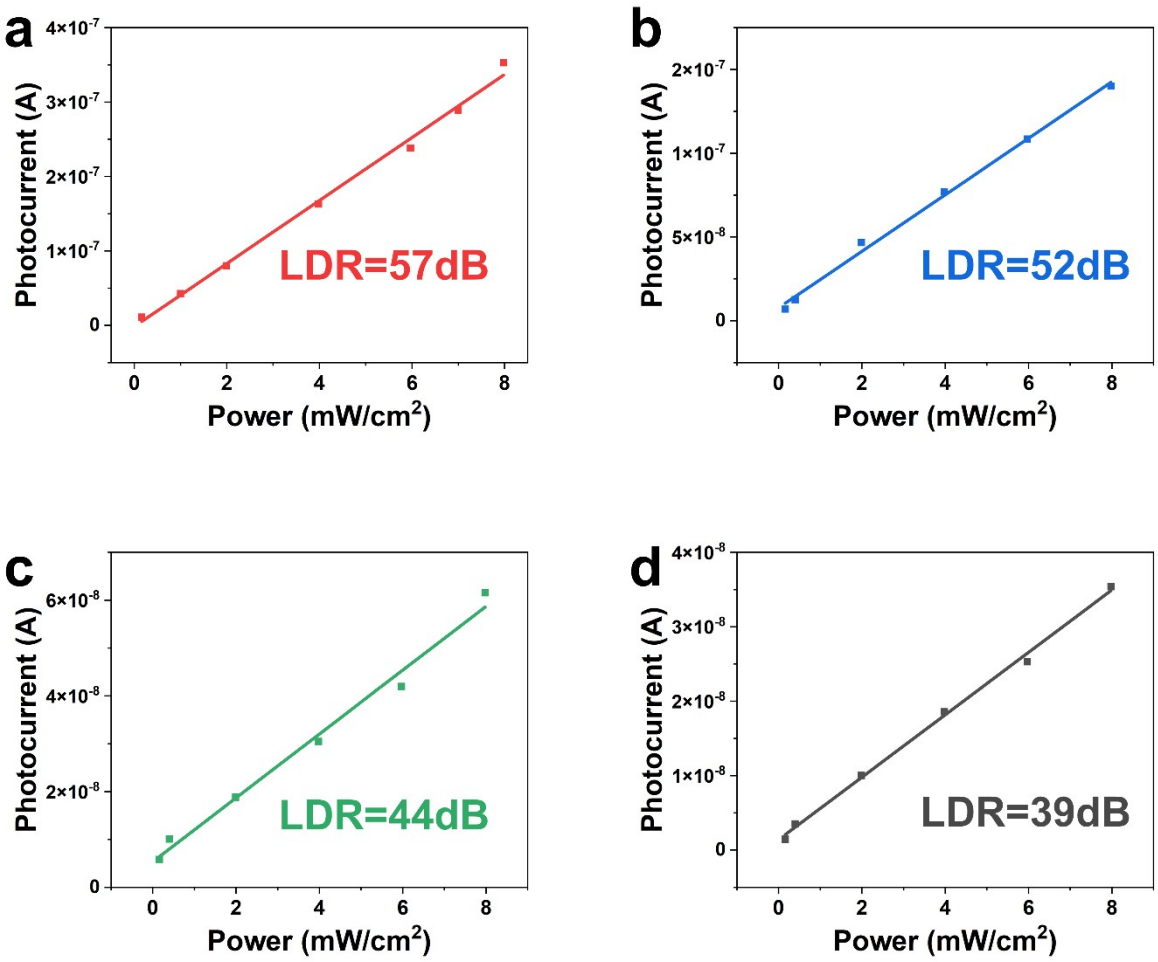

Figure S13. LDR of (a) 600 nm-PD, (b) 900 nm-PD, (c) 180 nm-PD and (d) Flat-PD at 5 V bias. 600 nm-PD has better photostability.

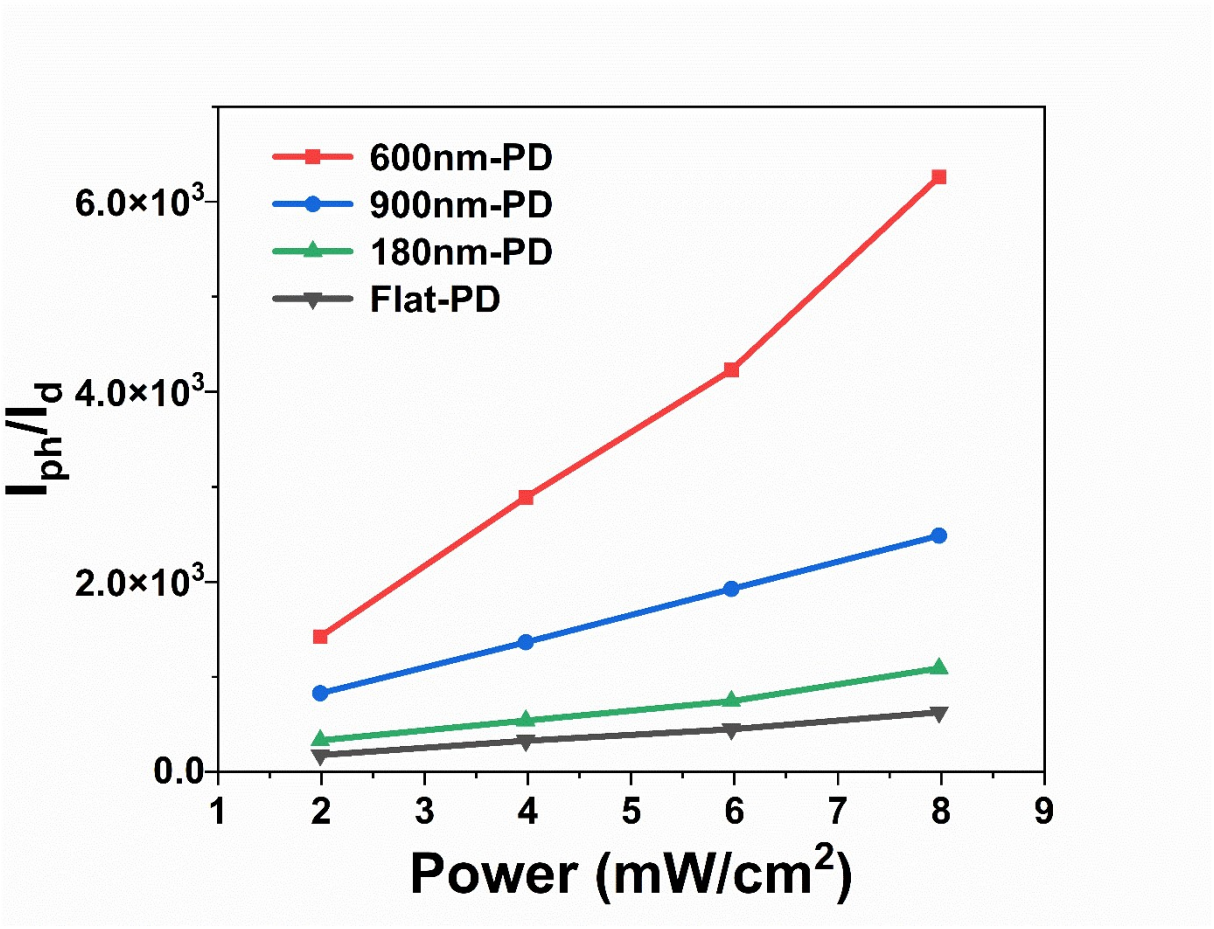

Figure S14. On/off ratio calculation of 600 nm-PD, 900 nm-PD, 180 nm-PD and Flat-PD at different incident light power.

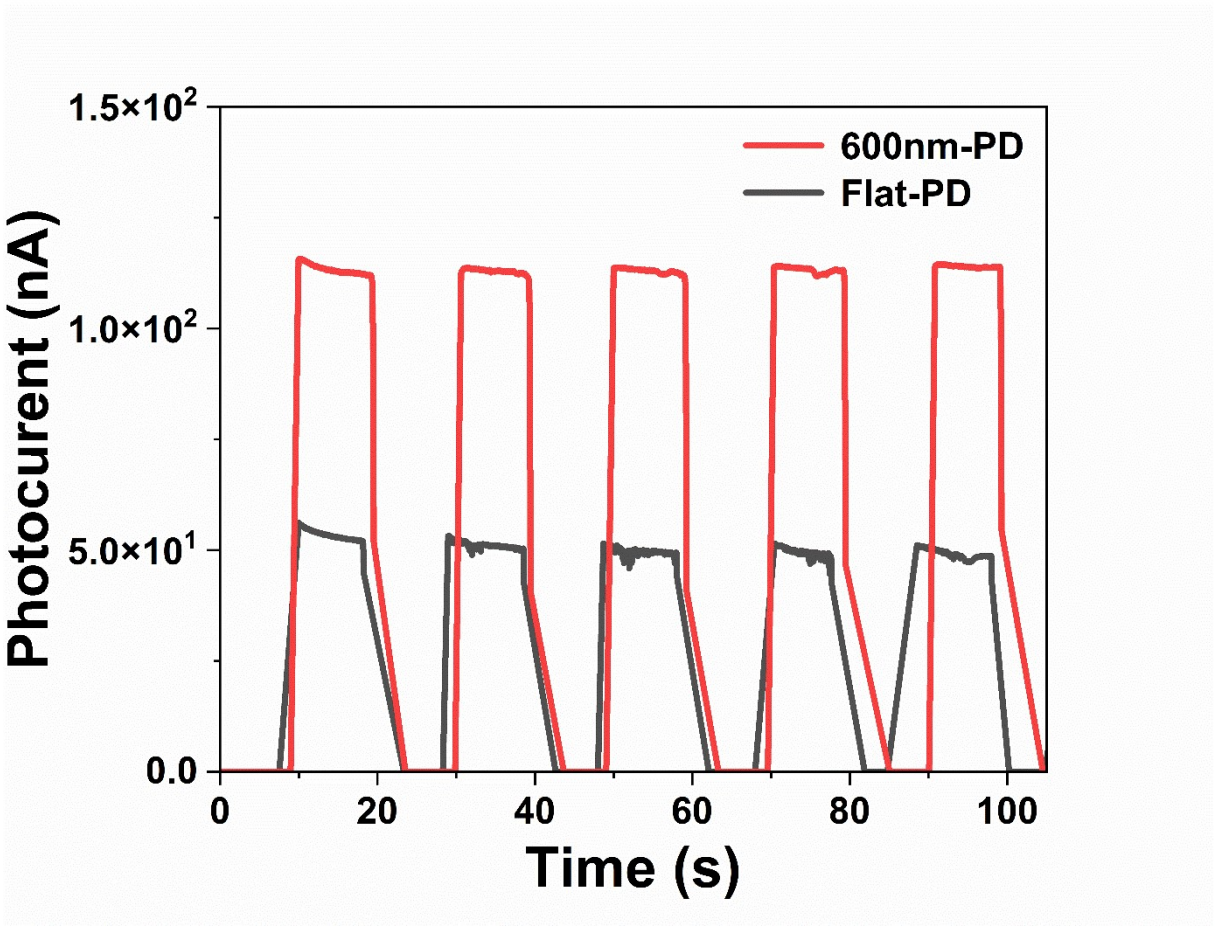

Figure S15. I-t curves of 600 nm-PD and Flat-PD in dark and under white light illumination at 5 V bias.

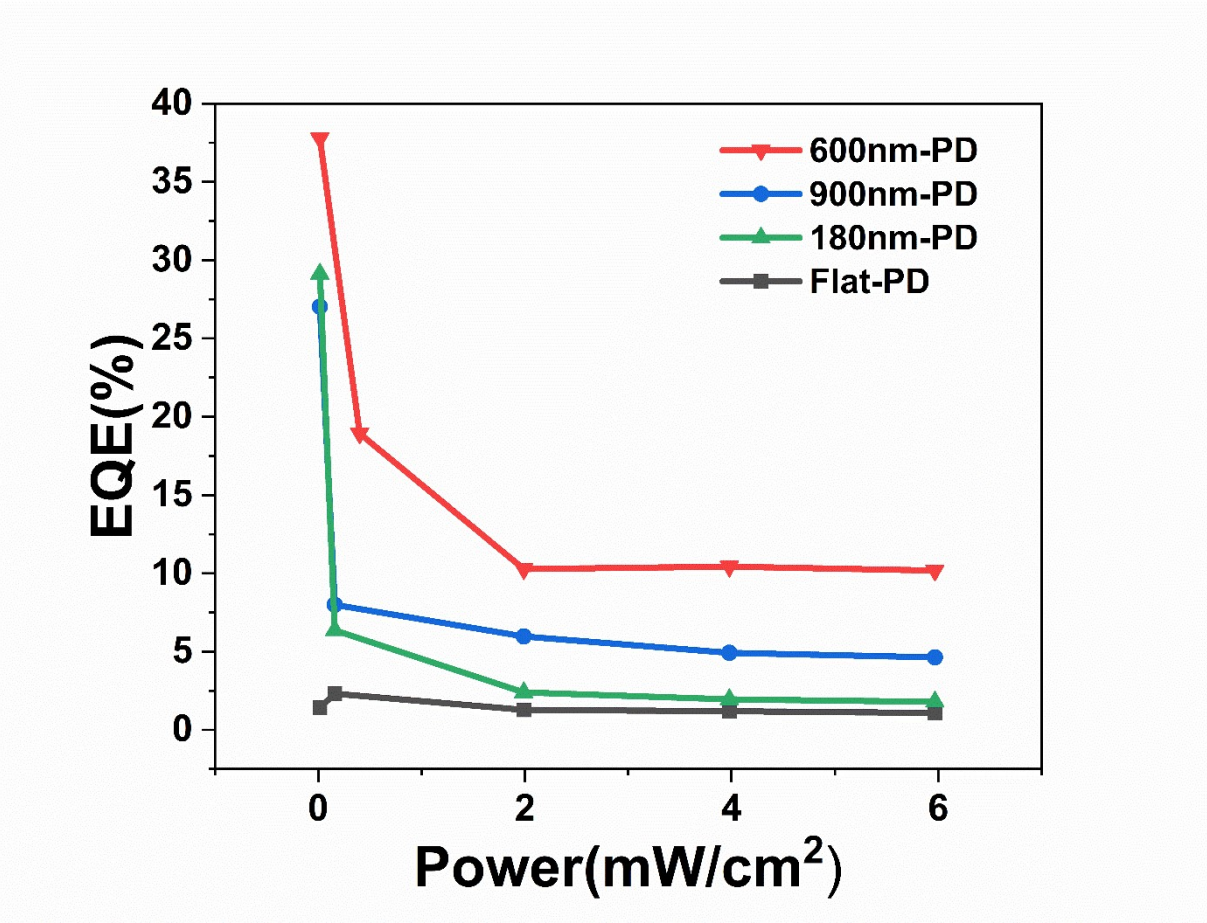

Figure S16. External quantum efficiency (EQE) of 600 nm-PD, 900 nm-PD, 180 nm-PD and Flat-PD at different incident light power.

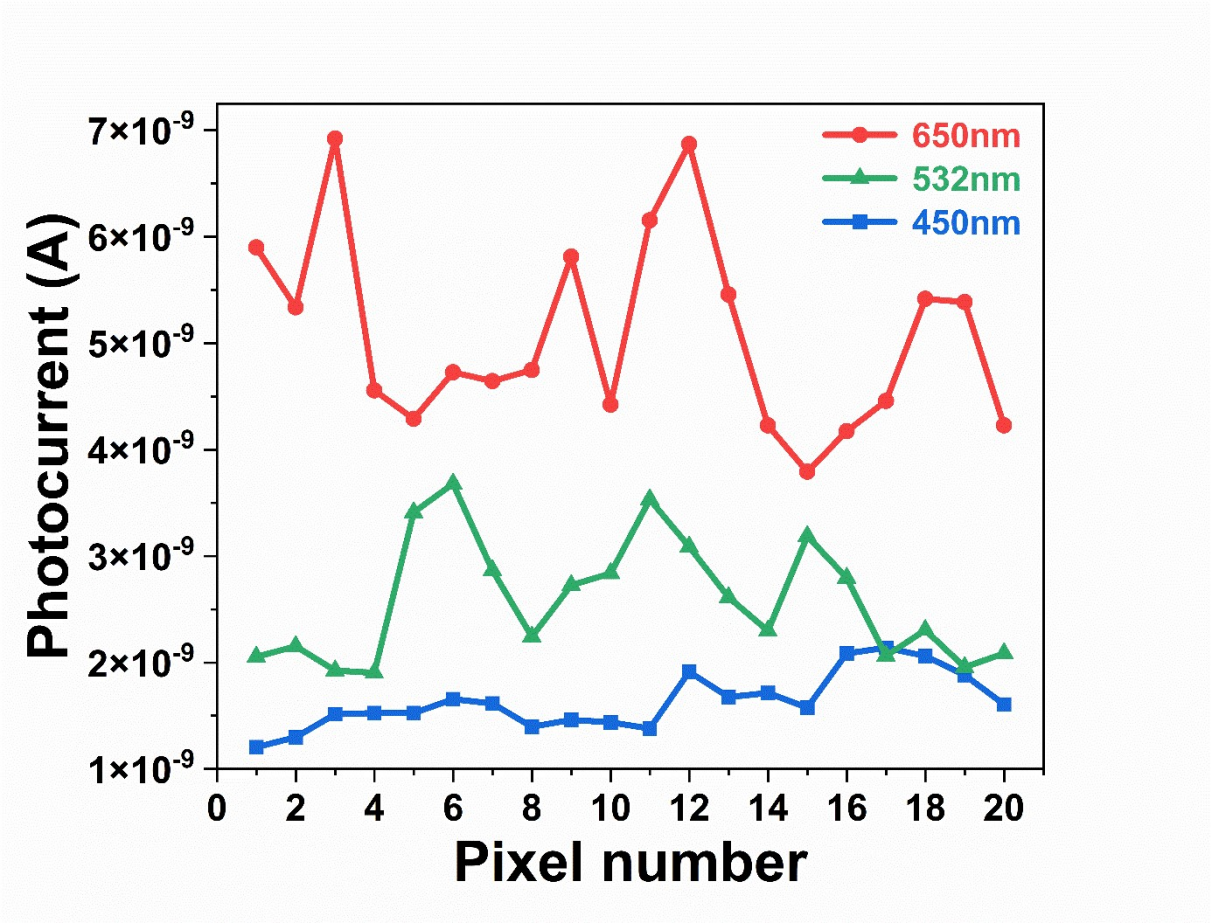

Figure S17. Photocurrent for 20 pixels of 600 nm-PD under the wavelength of 650 nm, 532 nm and 450 nm, respectively.

Table S1. Time-resolved photoluminescence of 600nm-PVK, 900nm-PVK, 180nm-PVK and Flat-PVK films.

Samples	T1 [ns]	T2 [ns]
600nm-PVK	47	258
900nm-PVK	79	214
180nm-PVK	67	179
Flat-PVK	42	140

Table S2. Comparison of the key parameters for $MAPbI_3$ based photodetectors.

Device structure	Detection condition	Perovskite structure	Responsivity [A W^{-1}]	Detectivity [Jones]	On/off ratio	Ref.
Au/$MAPbI_3$/Au	5V, 16μW cm^{-2}, 650nm light	Microsphere array	0.2	1.37×10^{13}	10^4	This work
Au/$MAPbI_3$/Au	10V, 100μW cm^{-2}, 650nm light	Nanowires	0.1	10^{12}	-	[1]
Au/$MAPbI_3$/Au	30V, 80μW cm^{-2}, 650nm light	Nanowires	1.3	2.5×10^{12}	23	[2]
ITO/$MAPbI_3$/ITO	10V, 100μW cm^{-2}, 650nm light	Microwires	1.2	2.39×10^{12}	10^4	[3]
Au/$MAPbI_3$/Au	White light	Nanonet	0.59	-	10^5	[4]
Au/$MAPbI_3$/Au	0V, 650nm light	Nanowires	0.0125	7.3×10^{12}	10^5	[5]
Au/$MAPbI_3$/Au	4V, 50μW cm^{-2}, 265nm light	Nanoflakes	12	10^{11}	10^4	[6]
Au/$MAPbI_3$/Au	2V, 38.5μW cm^{-2}, 650nm light	Nanoribbon	0.0389	8.21×10^{11}	-	[7]
C/$MAPbI_3$/CuO	550nm light	-	0.3717	1.65×10^{13}	371.7	[8]
Au/$MAPbI_3$/Au	1V, 10μW cm^{-2}, white light	Films	0.418	1.22×10^{13}	-	[9]
Au/$MAPbI_3$/Au	1V, 1μW cm^{-2}, 466/635nm light	Nanograting	3.23/6.2	-	10^3	[10]

Reference

[1] H. Deng, X. K. Yang, D. D. Dong, B. Li, D. Yang, S. J. Yuan, K. K. Qiao, Y. B. Cheng, J. Tang, H. S. Song, *Nano Lett.*,2015, **15**, 7963-7969.

[2] H. Deng, D. D. Dong, K. K. Qiao, L. L. Bu, B. Li, D. Yang, H. E. Wang, Y. B. Cheng, Z. X. Zhao, J. Tang, H. S. Song, *Nanoscale,* 2015, **7**, 4163-4170.

[3] Y. Liu, F. Li, C. Perumal Veeramalai, W. Chen, T. Guo, C. Wu, T. W. Kim, *ACS Appl. Mater. Interfaces*, 2017, **9**, 11662-11668.

[4] W. H. Wang, Y. R. Ma, L. M. Qi, *Adv. Funct. Mater.,* 2017, **27**, 1603653.

[5] F. R. Cao, W. Tian, M. Wang, H. P. Cao, L. Li, *Adv. Funct. Mater.*, 2019, **29**,1901280.

[6] W. Zheng, R. Lin, Z. Zhang, Q. Liao, J. Liu, F. Huang, *Nanoscale,* 2017, **9**, 12718-12726.

[7] S. Lim, M. Ha, Y. Lee, H. Ko, *Adv. Opt. Mater.* 2018, **6**, 1800615.

[8] H. Sun, W. Tian, F. Cao, J. Xiong, L. Li, *Adv. Mater.,* 2018, **30**, 1706986.

[9] S. F. Leung, K. T. Ho, P. K. Kung, V. K. Hsiao, H. N. Alshareef, Z. L. Wang, J. H. He, *Adv. Mater.,* 2018, **30**, 1704611.

[10] H. Wang, R. Haroldson, B. Balachandran, A. Zakhidov, S. Sohal, J. Y. Chan, A. Zakhidov, W. Hu, *ACS Nano,* 2016, **10**, 10921-10928.